

## Suppression of Interleukin-1 $\beta$ -Induced Nitric Oxide Production in RINm5F Cells by Inhibition of Glucose-6-phosphate Dehydrogenase<sup>†</sup>

Li Guo, Zhiquan Zhang, Katherine Green, and Robert C. Stanton\*

*Vascular Cell Biology, Joslin Diabetes Center and Harvard Medical School, One Joslin Place, Boston, Massachusetts 02215*

*Received May 10, 2002; Revised Manuscript Received October 11, 2002*

**ABSTRACT:** In rat pancreatic islets and insulin-producing cell lines, IL-1 $\beta$  induces expression of inducible nitric oxide synthase and NO production leading to impairment of glucose-stimulated insulin release and decreased cell survival. NADPH is an obligatory cosubstrate for iNOS synthesis of NO. We hypothesized that IL-1 $\beta$  stimulates an increase in activity of NADPH-producing enzyme(s) prior to NO production and that this increase is necessary for NO production. Using rat insulin-secreting RINm5F cells, we found that (1) IL-1 $\beta$  caused a biphasic change in the NADPH level (increased by 6 h and decreased after prolonged incubation in the presence of 2 ng/mL IL-1 $\beta$ ); (2) IL-1 $\beta$  stimulated increased activity of glucose-6-phosphate dehydrogenase (G6PD) in a time- and dose-dependent manner, and G6PD expression was increased by about 80% after exposure to 2 ng/mL IL-1 $\beta$  for 18 h; (3) IL-1 $\beta$ -stimulated NO production was positively correlated with increased G6PD activity; (4) IL-1 $\beta$  did not cause any significant change in enzyme activity of another NADPH-producing enzyme, malic enzyme; (5) IL-1 $\beta$ -induced NO production was significantly reduced either by inhibiting G6PD activity using an inhibitor of G6PD (dehydroepiandrosterone) or by inhibiting G6PD expression using an antisense oligonucleotide to G6PD mRNA; and (6) IL-1 $\beta$  stimulated a decrease in the cAMP level. 8-Bromo-cAMP caused decreased G6PD activity, and the protein kinase A inhibitor H89 led to a increase in G6PD activity in RINm5F cells. In conclusion, our data show that IL-1 $\beta$  stimulated G6PD activity and expression level, providing NADPH that is required by iNOS for NO production in RINm5F cells. Also, inhibition of the cAMP-dependent PKA signal pathway is involved in an IL-1 $\beta$ -stimulated increase in G6PD activity.

In type I diabetes mellitus, hyperglycemia is likely the outcome of a long-term negative balance between immune-mediated  $\beta$ -cell damage (1) and  $\beta$ -cell repair/regeneration (2). Cytokines are part of the armamentarium used by the immune system to destroy  $\beta$  cells (3–10). Under in vitro conditions interleukin-1 $\beta$  (IL-1 $\beta$ ), alone or in combination with tumor necrosis factor- $\alpha$  (TNF $\alpha$ ) or interferon- $\gamma$  (IFN $\gamma$ ), induces functional suppression and damage to rodent pancreatic islets (3, 11). Human islets are less sensitive to the deleterious effects of cytokines, but exposure of these islets for several days to the combination of IL-1 $\beta$  and TNF $\alpha$  and IFN $\gamma$  also induces  $\beta$ -cell functional impairment (12, 13) and islet-cell loss (14, 15).

Recent evidence points to the importance of the nitric oxide (NO)<sup>1</sup> radical as an effector molecule in IL-1 $\beta$ -induced  $\beta$ -cell damage. For example, IL-1 $\beta$  stimulates inducible NO synthase (iNOS) transcription and NO synthesis in islet cells (16), and analogues of L-arginine, the substrate of NO synthase, block the inhibitory action of IL-1 $\beta$  on islet insulin release (17–19). Two of the most important effects of NO

in rodent islets are (1) inactivation of the mitochondrial enzyme aconitase, a key enzyme in the Krebs cycle, thereby impairing glucose oxidation and cellular energy generation (20–22), and (2) induction of nuclear DNA damage (22–24).

NOSs require three cosubstrates (L-arginine, NADPH, and O<sub>2</sub>) and five cofactors [FAD, FMN, calmodulin, tetrahydrobiopterin (BH<sub>4</sub>), and heme] (25). NO production by NOS is critically dependent on the availability of the cosubstrates and cofactors. Previous work has shown that IL-1 $\beta$  stimulates BH<sub>4</sub> production prior to NO production in INS-1 rat pancreatic  $\beta$  cells (26). Although reducing substrate, or any cofactor, might limit NO production by iNOS, NADPH potentially has the central role in NO production since NADPH is an essential cosubstrate for iNOS and also a necessary cofactor for dihydrofolate reductase, dihydropteridine reductase, and sepiaterin reductase, which convert BH<sub>2</sub> to BH<sub>4</sub> (27).

NADPH is produced by malic enzyme (ME) and by the first two dehydrogenases of the pentose phosphate pathway (PPP), glucose-6-phosphate dehydrogenase (G6PD), the rate-limiting enzyme, and the next enzyme in the pathway, 6-phosphogluconate dehydrogenase (6PGD) (28–31). Recent work by us has demonstrated that stimulation of eNOS and NO production in endothelial cells can be altered by inhibition of G6PD, which reduces NADPH levels (27). Also, Corraliza et al. studied bone marrow macrophages and showed a parallel induction of G6PD and NO production,

<sup>†</sup> This work has been supported in part by a grant (DK-54380) from the NIDDK (to R.C.S.), a grant from the Adler Foundation (to L.G.), and a grant from the Juvenile Diabetes Foundation (to Z.Z.).

\* To whom correspondence should be addressed. Phone: (617) 732-2652. Fax: (617) 732-2637. E-mail: robert.stanton@joslin.harvard.edu.

<sup>1</sup> Abbreviations: AS, antisense oligonucleotide; DHEA, dehydroepiandrosterone; G6PD, glucose-6-phosphate dehydrogenase; iNOS, inducible nitric oxide synthase; ME, malic enzyme; NO, nitric oxide; PPP, pentose phosphate pathway; RINm5F, clonal rat insulinoma cells.

suggesting that NO production and G6PD activation are linked in these cells (32). Therefore, the present study was designed to investigate the relationship between NADPH-producing enzymes and IL-1 $\beta$ -induced NO production in a  $\beta$ -cell line, RINm5F cells. Our results show that IL-1 $\beta$  stimulated an increase in G6PD activity and expression level, and inhibition of G6PD activity or expression reduced IL-1 $\beta$ -induced NO production in RINm5F cells. Importantly, IL-1 $\beta$  did not cause any significant increase in activity of ME, which is thought to be the major source of NADPH in  $\beta$  cells. These results suggest that G6PD is the main source of NADPH for iNOS synthesis of NO following exposure of RINm5F cells to IL-1 $\beta$ .

## MATERIALS AND METHODS

**Materials.** 8-Bromoadenosine 3',5'-cyclic monophosphate, dehydroepiandrosterone (DHEA), glucose 6-phosphate, glucose-6-phosphate dehydrogenase, HEPES, sodium malate, *N*-(1-naphthyl)ethylenediamine dihydrochloride (NEDD), NADP, 6-phosphogluconic acid, 6-phosphogluconic acid dehydrogenase, sodium pyruvate, and sulfanilamide were obtained from Sigma. H-89 and *N*<sup>G</sup>-monomethyl-L-arginine (L-NMMA) were purchased from Calbiochem. RhIL-1 $\beta$  is the product of Promega. Rabbit anti-G6PD antibody was from Sigma. Rabbit anti-iNOS antibody was from Affinity Bioreagents, Inc. Fluorescein-conjugated anti-rabbit antibody was from Calbiochem. HRP-conjugated goat anti-rabbit IgG was from Bio-Rad.

**Cell Line and Cell Culture.** RINm5F cells were used between passages 25–35 and cultured in RPMI-1640 medium (without phenol red) supplemented with 20 mM glucose, 10% fetal bovine serum, 100 units/mL penicillin, 100  $\mu$ g/mL streptomycin (Life Technologies Inc.), 0.75 g/L NaHCO<sub>3</sub>, 10 mM HEPES, and 1 mM sodium pyruvate at 37 °C in a humidified atmosphere with 5% CO<sub>2</sub>. Also, all experiments were done using the other culture medium, M199 medium (without phenol red), which has an arginine concentration of 0.33 mM, since circulating arginine levels in rats are about 0.25–0.30 mM, and RPMI-1640 medium contains 1.2 mM arginine. Results were similar in both culture media. In addition, basal insulin secretion from RINm5F cells was measured. Results showed that the cells released insulin around 15 ng/10<sup>6</sup> cells in 90 min.

**Islet Isolation and Culture.** Islets were isolated from excised pancreas of male Sprague–Dawley rats (250 g) by collagenase digestion as described previously (33). Islets were cultured overnight in an atmosphere of 95% air and 5% CO<sub>2</sub> in CMRL-1066 tissue culture medium containing 5.5 mM glucose, 10% FBS, 100 units/mL penicillin, and 100  $\mu$ g/mL streptomycin.

**NADPH Measurement.** NADPH was measured as described by Zhang (34). In brief, the method is based on the fact that only NADH and NADPH (and not NAD<sup>+</sup> and NADP<sup>+</sup>) affect absorbance at 340 nm. An initial reading (*A*<sub>1</sub>) of cell extract at 340 nm measured total NADH and NADPH levels in the sample. An aliquot of the extract (100  $\mu$ L) was incubated at 25 °C for 5 min with glutathione reductase (5.0 IU) in 0.1 M phosphate buffer, pH 7.6, containing 5 mM glutathione (GSSG), 0.05 M EDTA, and 0.5% (v/v) Triton X-100. Absorbance at 340 nm was then measured (*A*<sub>2</sub>). NADPH levels were calculated as the difference between *A*<sub>1</sub> and *A*<sub>2</sub>.

**G6PD Activity Assay.** G6PD activity was determined, as already described (28), by measuring the rate of production of NADPH. Since 6-phosphogluconate dehydrogenase (6PGD), the second enzyme of PPP, also produces NADPH, both 6PGD and total dehydrogenase activity (G6PD + 6PGD) were measured separately as described in our previous research. G6PD activity was calculated by subtracting the activity of 6PGD from the total enzyme activity. Protein levels were determined for each sample using the Bio-Rad protein assay kit, and activity results were normalized by protein.

**Malic Enzyme Activity.** Malic enzyme activity was measured as described (35). Each cuvette contained 0.95 mL of 45 mM Tris buffer, pH 7.4, 0.6 mM sodium malate, 4.5 mM MgCl<sub>2</sub>, 0.5 mM NADP<sup>+</sup>, and 0.05 mL of cell lysate supernatant. Malate was added last and only after the formation of NADPH by endogenous cell substrates had reached a slow and uniform rate. Following the addition of malate, absorbance change was measured for 60 s and corrected for the rate of NADPH observed, prior to the addition of malate.

**Antisense Experiment.** Transfection was carried out as described in the instructions of the Sequitur, Inc., kit. In brief, RINm5F cells were washed once with Opti-MEM without serum or antibiotics. Then 26.4  $\mu$ L of oligofectin I (1 mg/mL) was added in 4 mL of Opti-MEM in a tube. In another tube 4.0  $\mu$ L of antisense oligonucleotide (100  $\mu$ M) was added to 1 mL of Opti-MEM. The two solutions were mixed together and allowed to sit at room temperature for 15 min. The mixture was added to cells and incubated at 37 °C in a humidified atmosphere with 5% CO<sub>2</sub> for 5 h. The medium was removed, Opti-MEM with 10% FBS was added to the cells, and the mixture was incubated for 24 h; cell treatments began thereafter. The antisense sequence was 5'-AGUAGUACCCACGUAGCCCACUGGGA-3'. Antisense transfection efficiency was assessed to be 70–80% by a fluorescent control oligomer (catalog no. 2013), which can be visualized ( $\lambda_{\text{ex}}$  = 494 nm,  $\lambda_{\text{em}}$  = 519 nm) using a fluorescence microscope (NiKon, AFX-DX).

**Nitrite Measurement.** NO synthesis was estimated by the accumulation of nitrite in RINm5F cell culture media. Nitrite in cell-free culture supernatants was measured as described by Ding et al. (36). Briefly, 0.05 mL of sample or standard (NaNO<sub>2</sub>) was mixed with 0.05 mL of Griess reagent, and absorbance was read at 550 nm after 10 min incubation at room temperature. The nitrite concentration was calculated from a NaNO<sub>2</sub> standard curve.

**Immunoprecipitation.** Immunoprecipitation was performed as described previously (37). RINm5F cells were harvested, washed three times with cold PBS (pH 7.4), and then lysed for 20 min on ice in 1 mL of lysis buffer: 0.1 M PBS containing 1% NP-40 and half a tablet of “complete” protease inhibitor cocktail (Roche Molecular Biochemicals). Cell lysate was divided into two equal 0.5 mL portions. Rabbit anti-iNOS antibodies (1:500 dilution) or both rabbit anti-G6PD (1:100 dilution) and mouse monoclonal to  $\beta$ -actin (1:500 dilution) antibodies were added to pair samples, and the lysates were incubated with rotation for 2 h at 4 °C. Forty microliters of protein A–Sepharose CL-4B (Amersham Pharmacia Biotech) was added to the antigen–antibody mixture, and the resultant mixture was incubated with rotation for 1 h at 4 °C. The protein A–Sepharose antibody complex

was isolated by centrifugation and washed three times with lysis buffer (0.5 mL/wash). The protein A–Sepharose antibody complex was then treated with 60  $\mu$ L of SDS gel loading buffer and boiled for 5 min to dissociate the protein A–Sepharose antibody complex. The supernatant was obtained by centrifugation and analyzed on 10% SDS–PAGE (38) followed by western blot.

**Western Blot Analysis.** Immunoprecipitates were separated by 10% SDS–PAGE and transferred to nitrocellulose membrane. Membranes were incubated in blocking buffer (PBS with 5% nonfat milk and 0.1% Tween 20) for 1 h at room temperature. Subsequently, the membranes were hybridized with rabbit anti-iNOS antibodies (1:1000 dilution), rabbit anti-G6PD (1:1500 dilution) antibodies, or mouse monoclonal to  $\beta$ -actin (1:1500 dilution) for 2 h at room temperature. After being washed three times for 10 min each with PBS containing 0.1% Tween 20, the membranes were incubated in HRP-conjugated goat anti-rabbit antibodies or goat anti-mouse antibody solution (1:2000 dilution) at room temperature for 1 h. Following antibody incubation, immunodetection was performed with the ECL–western blotting detection system (Amersham Pharmacia Biotech) according to the manufacturer's protocol.

**Immunofluorescence Assay.** RINm5F cells were harvested and seeded onto glass coverslips in 24-well plates (Falcon) to reach 70–80% confluence after 48 h. After RINm5F cells were exposed to IL-1 $\beta$  (2 ng/mL) for 12 h, cells were rinsed twice with PBS and fixed for 30 min with 1% paraformaldehyde/PBS. The cells were rinsed twice with PBS and then incubated with 1% Triton X-100 in PBS for 5 min. After being washed two times with PBS, the coverslips were blocked with 500  $\mu$ L of 2% BSA for 1 h at room temperature. The blocking solution was aspirated, and the cells were rinsed once with PBS. The coverslips were incubated with rabbit anti-G6PD antibodies at a dilution of 1:1000 in PBS for 1 h. The primary antibody was aspirated, and the cells were washed three times with PBS for 5 min each. After washing, the cells were incubated with fluorescein-conjugated anti-rabbit antibodies (1:400 dilution) for 1 h. The secondary antibody was removed, and the cells were washed three times with PBST (5 min each) and once with PBS. Coverslips then were mounted onto slides with Crystal Mount (Biomedica, Foster City, CA) and allowed to dry. Cells were examined using a confocal laser scan microscope, LSM 410 (Zeiss).

**Measurement of cAMP.** Cell lysates either from control cells or from cells exposed to IL-1 $\beta$  (2 ng/mL) for 6 h were prepared using lysis buffer. Then cAMP concentrations were determined using the cAMP kit TRK432 from Amersham Pharmacia Biotech according to the manufacturer's instructions. Isobutylmethylxanthine (IBMX, 1 mM) was included in all solutions to inhibit cAMP-dependent phosphodiesterase activity.

## RESULTS

**IL-1 $\beta$  Causes a Biphasic Change in the NADPH Level in RINm5F Cells.** In unstimulated RINm5F cells, NADPH was  $100 \pm 20$  pmol/ $10^7$  cells, as indicated by a dashed line in Figure 1A. Stimulation of the cells with 2 ng/mL IL-1 $\beta$  increased intracellular NADPH content after 3 and 6 h of incubation. Prolonged exposure to IL-1 $\beta$  resulted in a decrease of cellular NADPH content (Figure 1A, solid line).

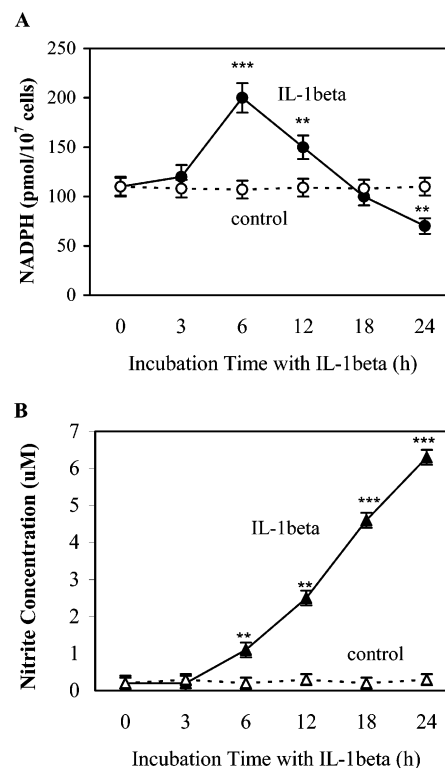


FIGURE 1: IL-1 $\beta$  affects NADPH level in a time-dependent manner in RINm5F cells. RINm5F cells (80–90% confluence) were exposed to 2 ng/mL of IL-1 $\beta$  for 0, 3, 6, 12, 18, and 24 h. The cells were harvested, and the cell lysates were used for the determination of NADPH content (A). The culture supernatants were collected for nitrite determination (B). Data are normalized by protein and presented as means  $\pm$  SE of three experiments: \*,  $p < 0.05$  vs control; \*\*,  $p < 0.005$  vs control; \*\*\*,  $p < 0.0005$  vs control.

Table 1: IL-1 $\beta$  Stimulates G6PD Activity in a Time-Dependent Manner in RINm5F Cells<sup>a</sup>

exposure time to IL-1 $\beta$ (h)	G6PD activity (% of control)
3	103 $\pm$ 1.6
6	125 $\pm$ 2.5 <sup>b</sup>
18	162 $\pm$ 3.4 <sup>b</sup>
24	175 $\pm$ 4.2 <sup>b</sup>
48	150 $\pm$ 3.2 <sup>b</sup>

<sup>a</sup> Data are normalized by protein and presented as means  $\pm$  SE ( $n = 3$ ). <sup>b</sup>  $p < 0.005$  vs control (without IL-1 $\beta$  treatment).

The decrease of intracellular NADPH levels after 6 h was accompanied by a continuous increase of nitrite accumulation (Figure 1B, solid line). The results suggest that the NADPH level rises as NADPH-producing enzyme(s) is (are) stimulated by IL-1 $\beta$ . Then NADPH levels decrease as newly synthesized iNOS utilizes NADPH.

**IL-1 $\beta$  Causes a Time- and Dose-Dependent Increase in G6PD Activity for RINm5F Cells.** Table 1 shows the time course of changes in G6PD activity stimulated by 2 ng/mL IL-1 $\beta$ . G6PD activity significantly increased following 6 h of exposure to IL-1 $\beta$ . With the time of exposure extended to 18 and 24 h, G6PD activity increased to about 162% and 175% of control, respectively, but no further increase was seen at 48 h of IL-1 $\beta$  treatment. Table 2 demonstrates the dose-dependent effect of IL-1 $\beta$  on G6PD activity. All concentrations of IL-1 $\beta$  tested proved to increase G6PD



Table 2: IL-1 $\beta$  Stimulates G6PD Activity and Nitrite Production in a Dose-Dependent Manner<sup>a</sup>

IL-1 $\beta$ concn (ng/mL)	G6PD activity (% of control)	nitrite production ( $\mu$ M)
0 (control)	100 $\pm$ 1.5	0.17 $\pm$ 0.01
0.5	154 $\pm$ 3.2 <sup>c</sup>	4.24 $\pm$ 0.10 <sup>d</sup>
1	171 $\pm$ 3.8 <sup>c</sup>	4.67 $\pm$ 0.14 <sup>d</sup>
2	163 $\pm$ 3.5 <sup>c</sup>	4.45 $\pm$ 0.11 <sup>d</sup>
4	126 $\pm$ 2.1 <sup>c</sup>	4.04 $\pm$ 0.17 <sup>d</sup>
8	114 $\pm$ 1.7 <sup>b</sup>	3.28 $\pm$ 0.12 <sup>c</sup>

<sup>a</sup> The values shown here are normalized by protein and presented as means  $\pm$  SE ( $n$  = 3). <sup>b</sup>  $p$  < 0.05 vs control. <sup>c</sup>  $p$  < 0.005 vs control. <sup>d</sup>  $p$  < 0.0005 vs control.

activity. The maximal stimulation of G6PD activity was reached at 1 ng/mL IL-1 $\beta$ .

Studies by Kwon et al. showed that IL-1 $\beta$  stimulates iNOS expression and NO production by rat islets and in  $\beta$ -cell lines (39). Consistent with the previous studies, the treatment of RINm5F for 18 h with 0.5–8 ng/mL IL-1 $\beta$  resulted in the dose-dependent production of NO. Importantly, the IL-1 $\beta$ -stimulated increase in NO production was positively correlated with increased G6PD activity.

*Malic Enzyme Activity Is Not Elevated in IL-1 $\beta$ -Stimulated RINm5F Cells.* MacDonald has reported that malic enzyme (ME) normally produces more NADPH than G6PD does in unstimulated  $\beta$  cells (29). However, our data show that ME activity was 1.17  $\pm$  0.12  $\mu$ mol/10<sup>7</sup> cells per minute ( $n$  = 3) after exposure of RINm5F cells to 2 ng/mL IL-1 $\beta$  for 18 h, and ME activity was 1.23  $\pm$  0.15  $\mu$ mol/10<sup>7</sup> cells per minute ( $n$  = 3) in unstimulated RINm5F cells. There is no significant change in ME activity after the treatment of IL-1 $\beta$ , while an 18 h exposure of 2 ng/mL IL-1 $\beta$  results in an approximate 30-fold increase in nitrite accumulation. Nitrite concentration was 0.17  $\pm$  0.02  $\mu$ M ( $n$  = 3) in unstimulated cells and 4.85  $\pm$  0.11  $\mu$ M ( $n$  = 3) in the IL-1 $\beta$ -stimulated cells. The above results suggest that G6PD, not ME, is the likely source of NADPH for the IL-1 $\beta$ -induced iNOS to produce NO in RINm5F cells.

RINm5F cells are transformed cells and may not reflect in vivo physiology. Thus we performed a few experiments in islets. First, islets were exposed to 2 ng/mL IL-1 $\beta$  for 18 h, and G6PD activity was found to increase by 10–20%. Importantly, IL-1 $\beta$  caused a 10–20% decrease in ME activity. Thus, as in RINm5F cells there is an increase in G6PD activity with no change or decrease in malic enzyme. Moreover, IL-1 $\beta$  caused an approximate 20-fold increase in nitrite accumulation in islets. Thus the IL-1 $\beta$ -stimulated increase in G6PD activity in islets is consistent with the RINm5F studies.

*IL-1 $\beta$ -Induced NO Production Is Reduced by Inhibition of G6PD Activity.* If NADPH produced by G6PD is required for IL-1 $\beta$ -stimulated NO production, then inhibition of G6PD should result in decreased NADPH and NO production. To determine if reduced G6PD activity influences NO production by iNOS, RINm5F cells were treated with dehydroepiandrosterone (DHEA), a noncompetitive inhibitor of G6PD. RINm5F cells were preincubated with 100  $\mu$ M DHEA for 2 h before exposure to 2 ng/mL IL-1 $\beta$  for an additional 18 h. It was found that DHEA caused a decrease in NADPH concentration from 110  $\pm$  12 pmol/10<sup>7</sup> cells to 76  $\pm$  10 pmol/10<sup>7</sup> cells. Also, IL-1 $\beta$ -stimulated nitrite accumulation

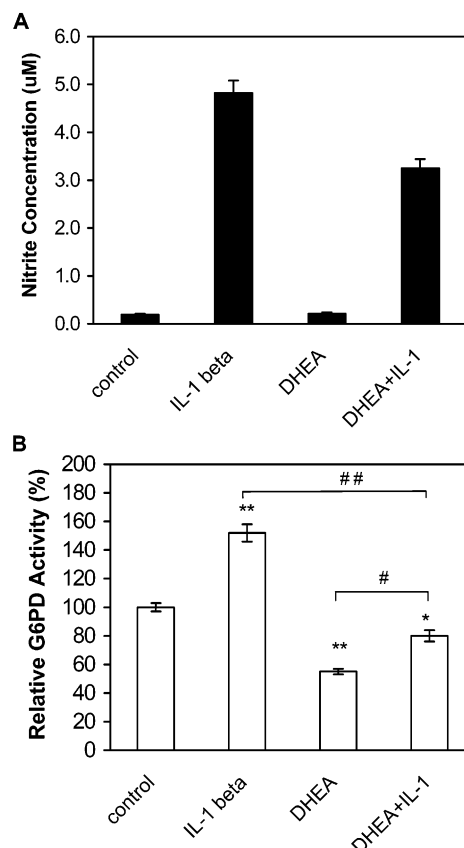
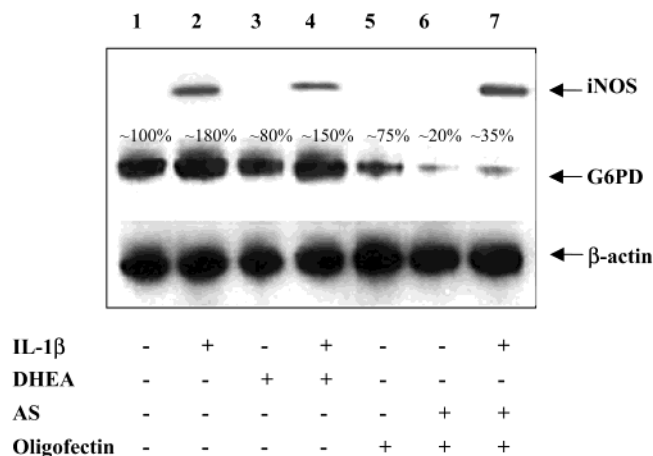


FIGURE 2: G6PD inhibitor DHEA reduces IL-1 $\beta$ -stimulated NO production in RINm5F cells. RINm5F cells were preincubated with 100  $\mu$ M DHEA for 2 h prior to exposure to 2 ng/mL IL-1 $\beta$  for an additional 18 h. The cell culture supernatants were collected for nitrite determination (A), and the cells were harvested for G6PD activity assay (B). The values are normalized by protein and presented as means  $\pm$  SE of three experiments: \*,  $p$  < 0.05 vs control; \*\*,  $p$  < 0.005 vs control; #,  $p$  < 0.05; ##,  $p$  < 0.005.

in RINm5F cells was significantly reduced by the G6PD inhibitor DHEA (Figure 2A). G6PD activity was decreased by about 45% after the treatment of DHEA (Figure 2B), as expected. Thus there is a clear correlation between NADPH levels and NO accumulation.

The effect of IL-1 $\beta$  on G6PD expression level was examined by immunoprecipitation and western blot. IL-1 $\beta$  stimulated an increase in G6PD protein expression by 80% (Figure 3, lane 2). Increased G6PD protein expression by IL-1 $\beta$  stimulation is possibly the reason IL-1 $\beta$ -stimulated G6PD activity was still higher than the control value after treatment with DHEA (Figure 2B).

In published experiments, DHEA has been shown to decrease IL-1 $\beta$ -induced nitrite accumulation in islets by nearly 50% (46). Since DHEA has possibly multiple actions and since oligonucleotide antisense transfection is not feasible in isolated islets, we did not simply repeat the published DHEA experiments in islets. Rather, we sought to determine whether glucose metabolism is required for IL-1 $\beta$  stimulation of NO, which should be the case if G6PD is involved. In the glucose removal experiments, islets were exposed to 2 ng/mL IL-1 $\beta$  in normal media for 15 h and then incubated in medium with or without 25 mM glucose in the presence of 2 ng/mL IL-1 $\beta$  for an additional 3 h. Glucose removal led to significant decreases in both the IL-1 $\beta$ -stimulated G6PD activity and nitrite accumulation in islets. These results



**FIGURE 3:** Western blot analysis of G6PD and iNOS expression in RINm5F cells. RINm5F cells (80–90% confluence) were treated by 2 ng/mL IL-1β alone for 18 h or in combination of DHEA or an AS against G6PD mRNA. Cells were preincubated with 100 μM DHEA for 2 h prior to exposure to 2 ng/mL IL-1β for an additional 18 h. Transfection with AS was performed as described in Materials and Methods. Following transfection, cells were exposed to 2 ng/mL IL-1β for 18 h. Cells were harvested after exposure to IL-1β. G6PD and iNOS were immunoprecipitated and identified by western blot as described in Materials and Methods. The membrane was then stripped, and ECL–western blot analysis was performed with a mouse monoclonal antibody against β-actin to verify the loading. Quantitation of G6PD protein was analyzed by ImageQuant software (Microsoft Corp.), which determines the average pixel value along the length of a rectangle. Numbers on the figure represent density analysis, with control equal to 100%.

support the critical role for glucose in IL-1β stimulation of NO production.

**IL-1β-Induced NO Production Is Diminished by Inhibition of G6PD Expression.** To further establish the role of G6PD in IL-1β-induced NO production by iNOS, G6PD expression was diminished by transfection with an antisense oligonucleotide against G6PD mRNA (AS). Following AS transfection, there was a significant reduction in G6PD protein expression (Figure 3, lanes 6 and 7) and in G6PD activity (Figure 4B) in RINm5F cells. Also, NADPH concentration was significantly diminished from  $110 \pm 12$  pmol/ $10^7$  cells to  $54 \pm 10$  pmol/ $10^7$  cells. Importantly, nitrite formation induced by IL-1β was significantly reduced in AS-transfected RINm5F cells as compared to cells treated by vehicle only (Figure 4A). This result confirms that G6PD activity is required for IL-1β-stimulated NO production by iNOS and confirms that there is a clear correlation between NADPH levels and NO accumulation.

In addition, DHEA and AS have little effect on the expression of iNOS induced by IL-1β (Figure 3, lanes 4 and 7). This demonstrates that DHEA and AS cause the reduced NO accumulation due to inhibition of G6PD and not due to effects on iNOS.

**IL-1β Stimulates Increased G6PD Activity Partly by Inhibition of the PKA Signal Pathway.** As noted in the introduction, published evidence shows that both G6PD and NOS can be regulated by PKA (40–42). Thus the effect of IL-1β on cAMP and PKA in RINm5F cells was studied. The cAMP basal level in RINm5F cells was  $38.6 \pm 1.5$  pmol/3 min per  $10^6$  cells ( $n = 3$ ). cAMP concentration was decreased to  $7.5 \pm 1.5$  pmol/3 min per  $10^6$  cells ( $n = 3$ ,  $p < 0.05$  versus basal level) after the exposure of RINm5F cells to 2

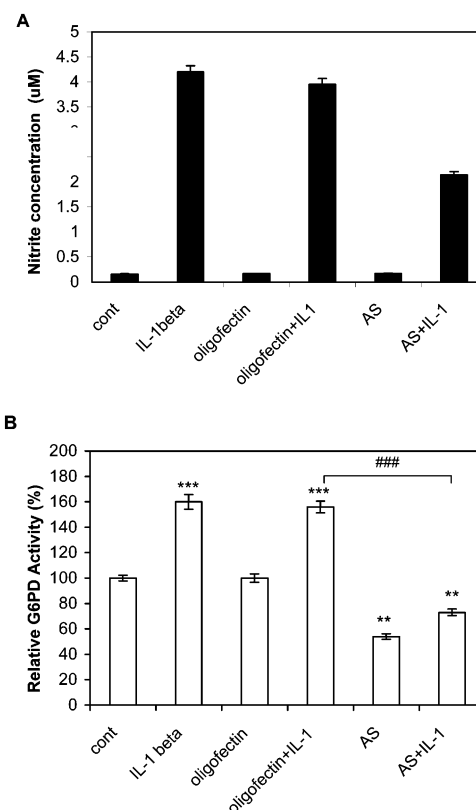


**FIGURE 4:** Inhibition of nitrite production by antisense oligonucleotide to G6PD mRNA in RINm5F cells. RINm5F cells (80–90% confluence) were transfected with an antisense oligonucleotide against G6PD mRNA (AS, 120 nM) as described in Materials and Methods. Following transfection, RINm5F cells were exposed to 2 ng/mL of IL-1β for 18 h. The culture supernatants were collected for nitrite determination (A), and the cells were harvested for G6PD activity assay (B). The values are normalized by protein and presented as means  $\pm$  SE from three experiments: \*\*,  $p < 0.005$  vs control; \*\*\*,  $p < 0.0005$  vs control; ###,  $p < 0.0005$ .

ng/mL IL-1β for 6 h. The data show that IL-1β caused a significant decrease in cAMP level in RINm5F cells, which is consistent with previous studies (43, 44). Previous work by us has shown that increased cAMP leads to inhibition of G6PD activity in endothelial cells (42). Taken together, we hypothesize that the IL-1β-stimulated increase in G6PD activity in RINm5F may be caused by the reduced cAMP level and the subsequent decrease in cAMP-dependent protein kinase A (PKA) activity in addition to the increase in G6PD protein expression. If decreased cAMP elevates G6PD activity, then the cAMP analogue like 8-bromo-cAMP should cause a decrease in G6PD activity. Figure 5 shows that 8-bromo-cAMP caused a decrease (nearly 20%) in G6PD activity and partially reversed the stimulation of IL-1β on G6PD activity, and 8-bromo-cAMP led to a decrease of about 18% in IL-1β-induced NO production. These results indicate that cAMP is involved in the stimulation of G6PD by IL-1β. Furthermore, RINm5F cells were treated with PKA inhibitor H89, and it was found that H89 led to an increase in G6PD activity in RINm5F cells, compared to control. However, there was only a nonsignificant trend to a higher IL-1β-stimulated nitrite accumulation or G6PD activity when IL-1β and H89 were combined (Figure 5). This result suggests that IL-1β maximally decrease PKA activity and that the addition of H89 has no additive effect. The above results suggest that inhibition of the cAMP-dependent PKA

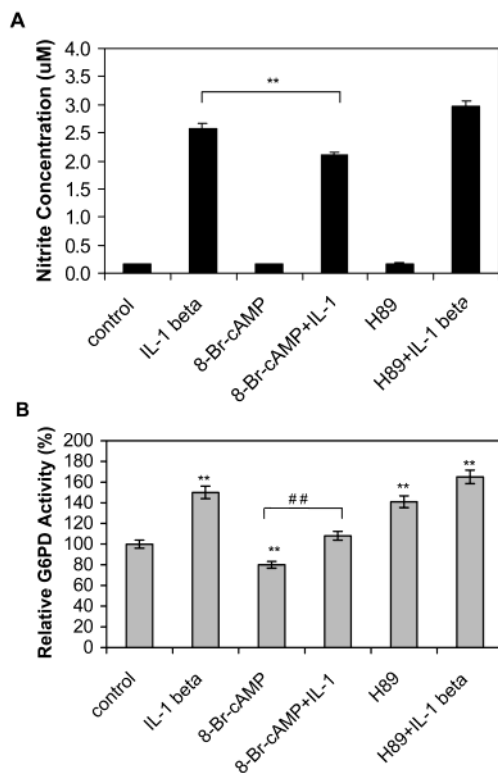


FIGURE 5: Effects of 8-bromo-cAMP and the PKA inhibitor H89 on G6PD activity in RINm5F cells. RINm5F cells (80–90% confluence) were incubated for 6 h in the absence or presence of 2 ng/mL IL-1 $\beta$ , with or without 0.5 mM 8-bromo-cAMP. For the H89 experiments, cells were preincubated with 20  $\mu$ M H89 for 45 min before exposure to 2 ng/mL IL-1 $\beta$  for an additional 6 h. The culture supernatants were collected for nitrite determination (A), and the cells were harvested for G6PD activity assay (B). Data represent means  $\pm$  SE of four individual experiments, performed in triplicate: \*\*,  $p < 0.005$  vs control; ##,  $p < 0.005$ .

signaling pathway is involved in the IL-1 $\beta$ -stimulated increase in G6PD activity.

**Effect of the NOS Inhibitor L-NMMA on G6PD Activity.** NO accumulation may compromise the cellular redox state via oxidation of thiols, such as glutathione (34). It has been shown that G6PD induction serves to maintain and regenerate the intracellular GSH pool by producing NADPH (45). Thus, it seemed possible that production of NO could affect G6PD activity. We examined the possibility that NO itself regulates G6PD activity in a feedback manner. L-NMMA, an inhibitor of NOS activity, was used to treat RINm5F cells. Figure 6A shows that IL-1 $\beta$ -stimulated nitrite production was hindered by the iNOS inhibitor L-NMMA. L-NMMA caused only a slight decrease in IL-1 $\beta$ -stimulated G6PD activity (Figure 6B). This suggests that G6PD activity is not significantly affected by IL-1 $\beta$ -stimulated NO accumulation at 18 h. Furthermore, as seen in Figure 6C, IL-1 $\beta$  stimulation of NADPH levels was back to baseline by 18 h, but, importantly, inhibition of iNOS by L-NMMA led to a highly significant increase in NADPH. This result confirms that iNOS utilizes NADPH for NO production and the NADPH level was decreased due to newly synthesized iNOS utilizing NADPH.

**IL-1 $\beta$  Stimulates Translocation of G6PD in RINm5F Cells.** The cellular localization of G6PD in RINm5F cells was examined by immunofluorescence confocal microscopy. After exposure of RINm5F cells to 2 ng/mL IL-1 $\beta$  for 12 h,

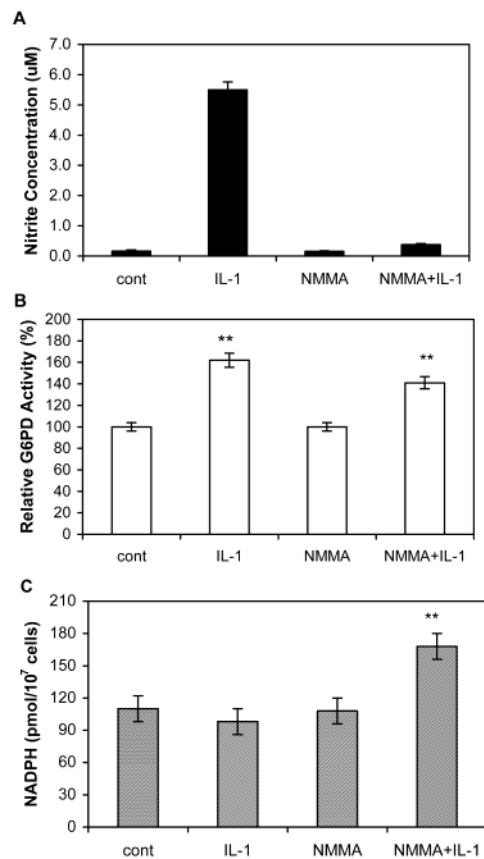


FIGURE 6: Effect of inhibition of iNOS by L-NMMA on G6PD activity and NADPH level. RINm5F cells (80–90% confluence) were treated with 2 ng/mL IL-1 $\beta$  alone, 0.5 mM L-NMMA alone, or 2 ng/mL IL-1 $\beta$  + 0.5 mM L-NMMA for 18 h. Cells were preincubated with the NOS inhibitor L-NMMA for 1 h before exposure to IL-1 $\beta$  for an additional 18 h. The values are normalized by protein and presented as means  $\pm$  SE from three experiments, performed in triplicate: \*\*,  $p < 0.005$  vs control.

the G6PD localization has clearly changed from a relatively diffuse staining to a localized staining that appears to be near the cell membrane (Figure 7). In addition, the signal intensity increases as well in the IL-1 $\beta$ -stimulated RINm5F cells, which is consistent with the above western blot analysis result that G6PD expression was increased by IL-1 $\beta$  stimulation in RINm5F cells. This indicates that IL-1 $\beta$  stimulation not only increases in G6PD activity and expression but also causes the translocation of G6PD in RINm5F cells.

## DISCUSSION

Cytokines are principal mediators of  $\beta$ -cell death (3–10), and NO clearly plays a role in  $\beta$ -cell damage and death (20–24). Although other factors are certainly involved, reducing the toxic effects of NO production will likely improve  $\beta$ -cell survival. The cytokine-stimulated induction of iNOS is paralleled by induction of other cytokine-dependent genes in  $\beta$  cells. Some of these genes may contribute to  $\beta$ -cell damage, while others are probably involved in  $\beta$ -cell defense and/or repair. Thus there are multiple possible approaches to regulating and preventing the deleterious effects of cytokine elaboration. In this paper we show that one enzyme, G6PD, plays a very important role in providing NADPH for iNOS activity and, thus, may represent an interesting target for manipulation of NO production. Inhibition of G6PD leads to a reduction in NADPH that has the potential of signifi-



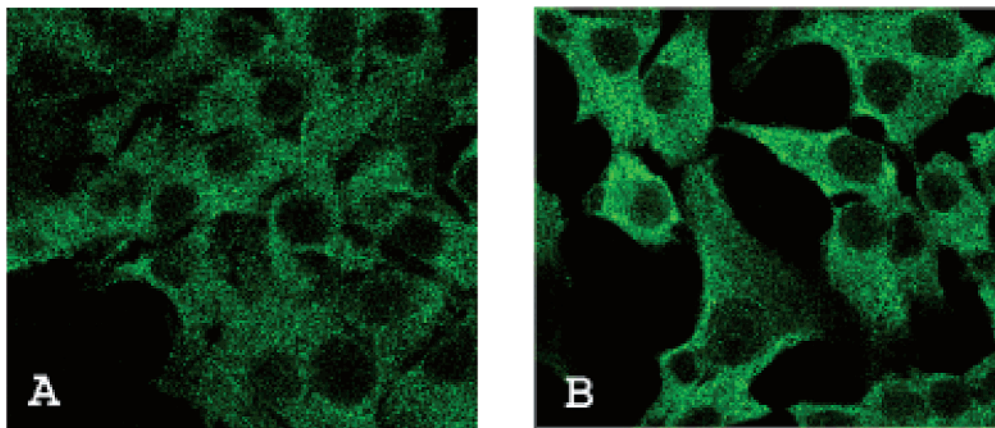


FIGURE 7: IL-1 $\beta$ -stimulated translocation of G6PD in RINm5F cell detected by confocal microscopy. Panel A shows the localization of G6PD in unstimulated RINm5F cells. Panel B shows the localization of G6PD in IL-1 $\beta$ -stimulated RINm5F cells.

cantly impairing NO production. This is because NADPH plays a uniquely important role as a cosubstrate for NOS, as NADPH is also a necessary cofactor for dihydrofolate reductase, dihydropteridine reductase, or sepiaterin reductase that produces BH<sub>4</sub> (27). Thus, two cofactors of iNOS are reduced, NADPH and BH<sub>4</sub>.

Evidence in this paper indicates that IL-1 $\beta$  induces an increase in G6PD activity in a time- and dose-dependent manner and also causes an increase in G6PD expression level by 80% in RINm5F cells. Results also indicate that inhibition of G6PD activity or expression causes reduction of IL-1 $\beta$ -induced nitrite accumulation. Nitrite formation in RINm5F cells in response to IL-1 $\beta$  was significantly reduced during exposure to the G6PD activity inhibitor DHEA, although nitrite levels were still elevated above control values. Taken together, these results strongly support the hypothesis that IL-1 $\beta$  stimulates G6PD. This result is consistent with previous studies by Laychock (46, 47), in which it was proposed that inhibition of glucose metabolism and pentose shunt activity may protect the cells from NOS activation and related toxicity. Laychock and colleagues also showed that DHEA prevented cytokine-stimulated NO production (47). However, DHEA, a 17-ketosteroid derived from pregnenolone, also serves as a precursor in testosterone synthesis, and it has multiple actions. Thus it is a useful tool, but it is not a specific inhibitor for G6PD. Therefore, we employed a highly specific antisense oligonucleotide against G6PD mRNA to inhibit G6PD expression. Importantly, specific antisense inhibition of G6PD led to a significant inhibition of IL-1 $\beta$ -stimulated nitrite accumulation in RINm5F cells. We believe that this result confirms that IL-1 $\beta$ -stimulated NO production requires NADPH provided by G6PD.

The IL-1 $\beta$ -induced biphasic change in NADPH level (increased by 6 h and decreased after prolonged incubation, Figure 1A) is in agreement with the following hypothesis. G6PD is stimulated initially by IL-1 $\beta$ , producing NADPH. Then NADPH is utilized by the newly synthesized iNOS protein that needs NADPH. Maximal NO synthesis occurs only after saturation of enzyme complex with NADPH cofactor, which is synthesized in advance. Note that G6PD activity is increased by 6 h (Table 1). NADPH content rises until sufficient iNOS is expressed with increased utilization of NADPH. Increased NO production by 12 h ultimately leads to a decrease in NADPH level (Figure 1). Further confirmation of iNOS utilization of NADPH was seen when

RINm5F cells were exposed to the iNOS inhibitor L-NMMA and IL-1 $\beta$  for 18 h. NO production was inhibited, yet NADPH levels remained elevated (Figure 6C).

NADPH is produced by ME and by the first two dehydrogenases of the PPP, G6PD, the rate-limiting enzyme, and the next enzyme in the pathway, 6PGD (28–31). It has been thought that ME is the principal source of NADPH in  $\beta$  cells under unstimulated conditions. Our data do not refute that idea. Our data do show that NADPH for IL-1 $\beta$ -stimulated NO production is mediated by increased G6PD activity and not ME, as no significant change in ME activity was observed. This suggests that, under specific biologic conditions, G6PD is an important source of NADPH in  $\beta$  cells.

It has been reported that the NOS-inductive IL-1 signal was antagonized by lipophilic cAMP analogues, and results for nitrite accumulation in RINm5F cells pointed to activating protein kinase C and inhibitory protein kinase A signaling pathways (34). That is, phorbol esters led to enhancement of NO production whereas cAMP analogues led to inhibition of NO synthesis. Thus considering these results and our previously published role of cAMP in regulating G6PD activity, which showed that increased cAMP caused a decrease in G6PD activity through the cAMP-dependent PKA pathway in endothelial cells (44), we hypothesized that IL-1 $\beta$  would lead to a decrease in cAMP and, thus, activation of G6PD. The results in this study demonstrated that IL-1 $\beta$  caused a significant decrease in cAMP levels, which is consistent with our hypothesis. In agreement with the hypothesis that cAMP regulates G6PD in  $\beta$  cells, our result of the experiment using the PKA inhibitor, H89, led to an increase in G6PD activity in RINm5F cells. The results suggest that, in addition to stimulation of increased G6PD expression, IL-1 $\beta$  induced an increase in G6PD activity, at least in part by decreasing cAMP via decreased activity of PKA.

Regulation of iNOS and other related genes in  $\beta$  cells is complex (48). There are important differences in iNOS regulation between rodent and human pancreatic islets. Clearly, future work needs to be done in isolated islets (both rat and human) and in animal models of immune-mediated pancreatic  $\beta$ -cell death. A detailed knowledge of the molecular regulation of these genes in  $\beta$  cells, as well as the physiologic interplay of these proteins, may be instrumental

in the development of new approaches to prevent  $\beta$ -cell destruction in early type I diabetes.

## ACKNOWLEDGMENT

We are very grateful to Drs. Joseph Loscalzo and Jane Leopold of the Boston University Medical Center for assistance in the antisense experiments. We thank Chris Cahill of Advanced Microscopy Core of the Joslin Diabetes Center for excellent technical assistance with confocal microscopy work.

## REFERENCES

- Bach, J. F. (1995) *J. Autoimmun.* 8, 439–463.
- Eizirik, D. L., Sandler, S., and Palmer, J. P. (1993) *Diabetes* 42, 1389–1391.
- Mandrup-Poulsen, T., Helquist, S., Wogensen, L., et al. (1990) *Curr. Top. Microbiol. Immunol.* 164, 169–193.
- Rabinovitch, A. (1993) *Diabetes Rev.* 1, 215–240.
- Andre-Schmutz, I., Hindelang, C., Benoist, C., and Mathis, D. (1999) *Eur. J. Immunol.* 29, 245–255.
- Ankarcrona, M., Dypbukt, J. M., Brune, B., and Nicotera, P. (1994) *Exp. Cell Res.* 213, 172–177.
- Corbett, J. A., Wang, J. L., Sweetland, M. A., Lancaster, J. R., Jr., and McDaniel, M. L. (1992) *J. Clin. Invest.* 90, 2384–2391.
- Costa, R. L.-F.B.P., Curi, R., Murphy, C., and Newsholme, P. (1995) *Biochem. J.* 310, 709–714.
- Messmer, U. K., and Brune, B. (1994) *Cell Signalling* 6, 17–24.
- Corbett, J. A., and McDaniel, M. L. (1995) *J. Exp. Med.* 181, 559–568.
- Sandler, S., Eizirik, D. L., Svensson, C., Strandell, E., Welsh, M., and Welsh, N. (1991) *Autoimmunity* 10, 241–253.
- Corbett, J. A., Sweetland, M. A., Wang, J. L., et al. (1993) *Proc. Natl. Acad. Sci. U.S.A.* 90, 1731–1735.
- Eizirik, D. L., Sandler, S., Welsh, N., et al. (1994) *J. Clin. Invest.* 93, 1968–1974.
- Eizirik, D. L., Sandler, S., Welsh, N., et al. (1994) *Autoimmunity* 19, 193–198.
- Rabinovitch, A., Suarez-Pinzon, W. L., Strynadka, K., et al. (1994) *J. Clin. Endocrinol. Metab.* 79, 1058–1062.
- Eizirik, D. L., Cagliero, E., Björklund, A., and Welsh, N. (1992) *FEBS Lett.* 308, 249–252.
- Southern, C., Schulster, D., and Green, I. C. (1990) *FEBS Lett.* 276, 42–44.
- Welsh, N., Eizirik, D. L., Bendtzen, K., et al. (1991) *Endocrinology* 129, 3167–3173.
- Corbett, J. A., Lancaster, J. R., Jr., Sweetland, M. A., et al. (1991) *J. Biol. Chem.* 266, 21351–21354.
- Welsh, N., Eizirik, D. L., Bendtzen, K., and Sandler, S. (1991) *Endocrinology* 129, 3167–3173.
- Eizirik, D. L., Welsh, N., Niemann, A., et al. (1994) *FEBS Lett.* 337, 298–302.
- De-Mello, M. A., Flodstrom, M., and Eizirik, D. L. (1996) *Biochem. Pharmacol.* 52, 1703–1709.
- Delaney, C. A., Green, M. H. L., Lowe, J. E., and Green, I. C. (1993) *FEBS Lett.* 333, 291–295.
- Fehsel, K., Jalowy, A., Qi, S., et al. (1993) *Diabetes* 42, 496–500.
- Nathan, C., and Xie, Q. W. (1994) *Cell* 78, 915–918.
- Laffranchi, R., Schoedon, G., Blau, N., and Spinas, G. A. (1997) *Biochem. Biophys. Res. Commun.* 233, 66–70.
- Leopold, J., Cap, A., Scribner, A. W., et al. (2001) *FASEB J.* 15, 1771–1773.
- Tian, W., Braunstein, L. D., Pang, J., and Stanton, R. C. (1998) *J. Biol. Chem.* 273, 10609–10617.
- MacDonald, M. J. (1995) *J. Biol. Chem.* 270, 20051–20058.
- Jesaitis, A. J., and Allen, R. A. (1988) *J. Bioenerg. Biomembr.* 20, 679–707.
- Tian, W. N., Pignatere, J. N., and Stanton, R. C. (1994) *J. Biol. Chem.* 269, 14798–14805.
- Corraliza, J. M., Campo, M. L., Fuentes, J. M., et al. (1993) *Biochem. Biophys. Res. Commun.* 196, 342–347.
- McDaniel, M. L., Colca, J. R., Kotagal, N., and Lacy P. E. (1983) *Methods Enzymol.* 98, 182–200.
- Zhang, Z., Yu, J., and Stanton, R. C. (2000) *Anal. Biochem.* 285, 163–167.
- Wise, E. M., Jr., and Ball, E. G. (1964) *Biochemistry* 52, 1255–1262.
- Ding, A. H., Nathan, C. F., and Stuehr, D. J. (1988) *J. Immunol.* 141, 2407–2412.
- Springer, T. A. (1991) *Current Protocols in Molecular Biology*, Vol. 2, Green Publishing Associates and Wiley-Interscience, New York.
- Laemmli, U. K. (1970) *Nature* 227, 680–685.
- Kwon, G., Corbett, S. H., Hill, J. R., et al. (1998) *Diabetes* 47, 583–591.
- Messmer, U. K., and Brune, B. (1994) *Cell Signalling* 6, 17–24.
- Ishibashi, T., Godecke, A., and Schrader, J. (2001) *Tohoku J. Exp. Med.* 194, 75–90.
- Zhang, Z., Apse, K., Pang, J., and Stanton, R. C. (2000) *J. Biol. Chem.* 275, 40042–40047.
- Sandler, S., Bendtzen, K., Eizirik, D. L., et al. (1990) *Immunol. Lett.* 26, 245–252.
- Sjoholm, A. (1991) *FEBS Lett.* 289, 249–252.
- Salvemini, F., Franzé, A., Iervolino, A., et al. (1999) *J. Biol. Chem.* 274, 2750–2757.
- Laychock, S. G., and Bauer, A. L. (1996) *Endocrinology* 137, 3375–3385.
- Laychock, S. G. (1998) *Biochem. Pharmacol.* 55, 1453–1464.
- Eizirik, D. L., Flodstrom, M., Karlén, A. E., and Welsh, N. (1996) *Diabetologia* 39, 875–890.

BI026110V